Enzyme Kinetic Measurements Using a Droplet-Based Microfluidic System with a Concentration Gradient

ARTICLE *in* ANALYTICAL CHEMISTRY · MARCH 2011

Impact Factor: 5.64 · DOI: 10.1021/ac102472a · Source: PubMed

6 AUTHORS, INCLUDING:

Minh-Phuong Ngoc Bui
University of Minnesota Twin Cities
26 PUBLICATIONS **386** CITATIONS

SEE PROFILE

Jaebum Choo
Hanyang University
207 PUBLICATIONS **4,907** CITATIONS

SEE PROFILE

analytical chemistry

ARTICLE

pubs.acs.org/ac

Enzyme Kinetic Measurements Using a Droplet-Based Microfluidic System with a Concentration Gradient

Minh-Phuong Ngoc Bui,[†] Cheng Ai Li,[†] Kwi Nam Han,[†] Jaebum Choo,[†] Eun Kyu Lee,[‡] and Gi Hun Seong*[,†]

[†]Department of Bionano Engineering, Hanyang University, Ansan 426-791, South Korea

[‡]College of Bionanotechnology, Kyungwon University, Seongnam 461-701, South Korea

Supporting Information

ABSTRACT: In this paper, we propose a microfluidic device that is capable of generating a concentration gradient followed by parallel droplet formation within channels with a simple T-junction geometry. Linear concentration gradient profiles can be obtained based on fluid diffusion under laminar flow. Optimized conditions for generating a linear concentration gradient and parallel droplet formation were investigated using fluorescent dye. The concentration gradient profile under diffusive mixing was dominated by the flow rate at sample inlets, while parallel droplet formation was affected by the channel geometry at both the inlet and outlet. The microfluidic device was experimentally characterized using optimal layout and operating conditions selected through a design process. Furthermore, in situ enzyme kinetic measurements of the β-galactosidase-catalyzed hydrolysis of resorufin-β-D-galactopyranoside were performed to demonstrate the application potential of our simple, time-effective, and low sample volume microfluidic device. We expect that, in addition to enzyme kinetics, drug screening and clinical diagnostic tests can be rapidly and accurately performed using this droplet-based microfluidic system.

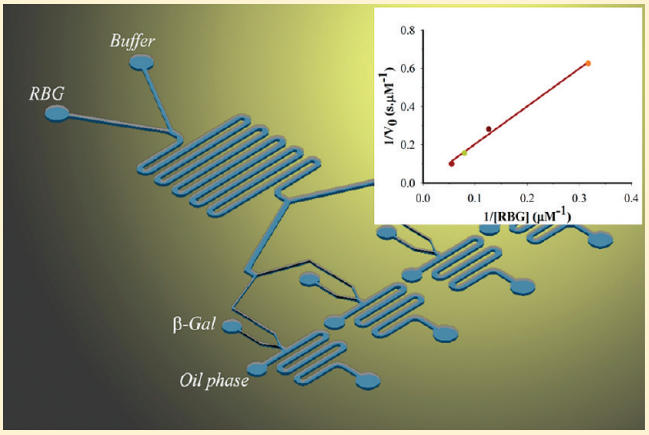

Droplet-based microfluidic systems are highly promising tools for a range of analytical and chemical processes. With the use of a droplet-based microfluidic platform, (i) a large number of reactions can be performed without increasing the device size or complexity, (ii) independent control of each droplet can be achieved, unlike in continuous-flow systems, and (iii) reactions can occur rapidly due to short mass transfer times and diffusion distances. Several research groups have reported the use of droplet-based microfluidic systems to directly synthesize particles and encapsulate various biological molecules for biotechnology applications.[1−4] In our previous study,[5] we have reported a technique for manufacturing polymeric microparticles containing enzymes that exploits the hydrodynamic behaviors of immiscible liquids in microfluidic systems and in situ photopolymerization. This technique allows for the simultaneous and continuous manufacturing of microbeads and the immobilization of enzymes.

In most microfluidic systems, reactions cannot be performed in parallel as well as in series, even thought this would be advantageous for monitoring reaction kinetics or for array studies of biological and biochemical systems.[6−8] However, reaction kinetic measurements should be performed via a series of experiments with different substrate concentrations. To achieve different substrate concentrations in microfluidic systems, a gradient generator is usually employed to generate and maintain a predictable concentration gradient of the sample over long periods of time. Several methods for generating concentration gradients have been developed, such as micropipets, hydrogel gradients, Boyden chambers, Zig-mond chambers, and Dunn chambers.[9−11] Among the methods, concentration gradients created under diffusive mixing have been shown to be stable for long periods of time, are easy to handle and fabricate, and have a simple design.[12−14] Laminar flow in a microfluidic system permits multiple streams of solution containing different concentrations to slowly diffuse while moving along the microchannel.[15−17] A stable gradient concentration can be achieved using multifluidic-based concentration gradient generators called multistep dividers.[12,18,19] These systems are able to generate linear, logarithmic, and parabolic gradient concentration profiles by altering the concentrations at the inlet channels. Another approach for generating a concentration gradient is to adjust the flow rates at the inlet channels of the T-junctions in a microfluidic device.[20] Multiple concentration gradient profiles such as linear, exponential, overlapping, and complex gradient profiles can be generated in a simple microfluidic device using hydrodynamic focusing.[21]

Received: September 18, 2010
Accepted: January 10, 2011
Published: January 31, 2011

In this study, we propose a droplet-based microfluidic device that uses diffusive mixing under laminar flow to generate a linear concentration gradient followed by parallel droplet formation in microchannels with a standard T-junction geometry. The developed device is capable of producing parallel droplets with different substrate concentrations for use in enzyme kinetic measurements. We determined the optimal parameters for obtaining a linear concentration gradient and stable droplet formation using a fluorescent dye as a model. Furthermore, to investigate the real-life application of the microfluidic device, enzyme kinetic measurements of the β-galactosidase-catalyzed hydrolysis of resorufin-β-D-galactopyranoside were performed.

EXPERIMENTAL SECTION

Materials. 1*H*,1*H*,2*H*,2*H*-Perfluorooctyl-trichlorosilane was obtained from Fluka Chemical Co. (Milwaukee, WI). 1*H*,1*H*,2*H*,2*H*-Perfluoro-1-octanol (PFO), perfluorodecalin (PFD), fluorescein isothiocyanate (FITC), resorufin-β-D-galactopyranoside (RBG), β-galactosidase (β-Gal), toluene, and resorufin were purchased from Sigma-Aldrich Chemical Co. (St. Louis, MO). Phosphate-buffered saline (PBS, pH 7.2) buffer was obtained from Biosesang Inc. (Sungnam, South Korea). Poly(dimethylsiloxane) (PDMS) prepolymer components (Sylgard 184 Silicon Elastomer Kit) were purchased from Dow Corning (Midland, MI). Microslide glass (no. S9213) was obtained from Matsunami Glass Ind. (Osaka, Japan).

Fabrication of the Microfluidic Device. The microfluidic device was fabricated based on PDMS using rapid prototyping and soft lithography, as described in our previous studies.[12,18] Briefly, a transparency mask generated by a 25 000 dpi high-resolution printer was used in photolithography with positive photoresist (AZ-P4620) to generate a master (10 μm thickness) template on the glass surface. After the PDMS had cured, the inlets and outlets of the channel were punched out using a sharpened needle tip (500 μm-diameter holes). The surface of the PDMS replica and a clean glass substrate were activated in air plasma prior to sealing. The PDMS surface channels were incubated in an oven at 120 °C for over 2 h to regenerate uniformly hydrophobic channel surfaces, followed by treatment with a solution of 1% 1*H*,1*H*,2*H*,2*H*-perfluorooctyl-trichlorosilane in toluene through the channels. The microfluidic device was then baked at 80 °C for 2 h before use.

Enzyme Kinetic Measurements. The microfluidic device was operated by controlling three individual syringe pumps (PHD2000, Harvard Apparatus, Holliston, MA). Teflon tubes (Cole-Parmer Instrument Co., Vernon Hills, IL) were used to connect the microfluidic device with the syringes. In total, 50 units/mL of β-Gal in PBS buffer and the carrier fluid (mixture of PFD and PFO at a ratio of 10:1, respectively) were used for β-Gal kinetic measurements. Droplets were observed using fluorescent microscopy (Olympus IX71) and a 10× objective at room temperature. A high-speed camera (Photometrics Coolsnap CF, Roper Scientific) was used for fluorescence imaging of droplets, as well as to determine the gradient concentration. To determine the height of the fluorescent peak, the data were first filtered to reduce the effect of noise before processing. The fluorescent intensity of each droplet was averaged, and the standard deviation was calculated. All images were captured using a 5 ms exposure time and were analyzed using Image-Pro Express v4.5 (Media Cybernetics Inc.).

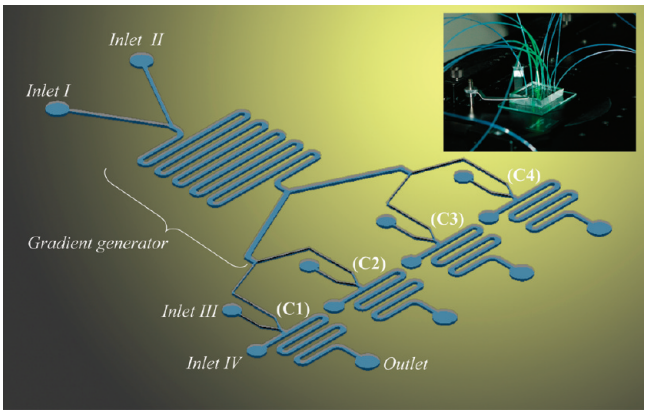

Figure 1. Schematic diagram of the droplet-based microfluidic device. The inset photograph shows the experimental setup with fluorescent microscopy and three syringe pumps.

RESULTS AND DISCUSSION

Gradient Generation in the Microfluidic Device. Our approach for generating a concentration gradient relies on mixing via lateral diffusion in a laminar flow regime.[22] Figure 1 shows a schematic of the microfluidic network used to generate a concentration gradient and the formation of parallel droplets in the T-junctions of a microfluidic device. The system consists of reservoirs, a winding channel that branches off into four downstream channels, and a parallel T-junction geometry channel for droplet formation. Two reservoirs on the top of the microfluidic device contain substrate (inlet I) and buffer (inlet II) solutions, respectively, and the concentration gradient is generated as the two fluids travel along the winding channel. The extent of sample mixing determines the shape of the resulting concentration profile, which evolves a smoother distribution as the sample migrates downstream. As a result, at the end of the channel, an approximately linear concentration profile can be obtained at the cross-section of the channel.

In a simple Y-junction microfluidic device, interfacial diffusion is dependent on the flow rate, the channel length, the diffusion coefficient of dissolved molecules, the viscosity of the fluid, and so on (Supporting Information).[16,23] We designed our microfluidic system to generate a linear concentration gradient depending on the flow rate of the injected solution at the reservoirs. The concentration gradient in this device was visualized and quantified using the fluorescent molecule fluorescein isothiocyan ate (FITC) as a model. To investigate the effect of flow rate on the distribution of FITC (1 mM), the pump was operated at several speeds, varying from 0.5 to 3 μL min^{-1} (Figure 2A). The FITC concentration was highest in channel one and was reduced in channel four (C1−C4). The most linear concentration gradient profile was observed at FITC flow rates of 1.0 μL min^{-1} (Figure S1 in the Supporting Information). Figure 2B shows fluorescent images of FITC in the four channels of the device at a flow rate of 1.0 μL min^{-1}.

Parallel Droplet Formation in the Microfluidic Device. In channels with standard T-junction geometries, droplet formation occurs at low values of the dimensionless capillary number,

$$\mathrm{Ca} = \frac{U\mu}{\gamma} \quad (1)$$

where U (meter second^{-1}) is the flow velocity, μ (kilogram

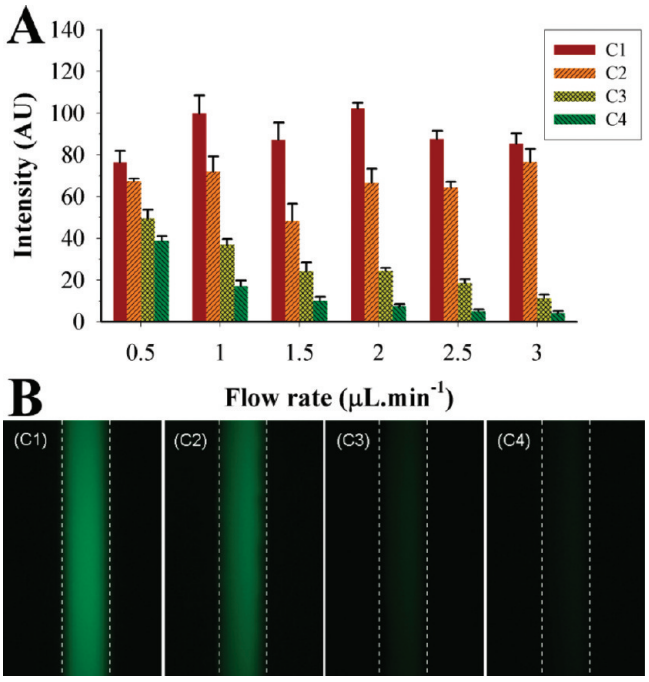

Figure 2. (A) The concentrations at different positions in the channel as a function of the flow rate ($V_{\text{inlet III (PBS)}}$ = 0.5 μL min^{-1} and $V_{\text{inlet IV (oil)}}$ = 1.0 μL min^{-1}, respectively). (B) Fluorescence images of the FITC concentration gradient in the four channels ($V_{\text{inlet I (FITC)}}$ = $V_{\text{inlet II (PBS)}}$ = 1.0 μL min^{-1}; $V_{\text{inlet III (PBS)}}$ = 0.5 μL min^{-1}, $V_{\text{inlet IV (oil)}}$ = 1.0 μL min^{-1}).

meter^{-1} second^{-1}) is the dynamic viscosity of the fluid, and γ (kilogram second^{-2}) is the surface tension at the interface between the aqueous phase and the carrier fluid.[24,25] While the typical processes of droplet formation in channels with a single T-junction geometry have been studied and are described in detail elsewhere,[26] we considered parallel droplet formation in several channels with a T-junction geometry. The length of droplets can be controlled according to the water fraction values (wf),

$$\text{wf} = \frac{V_w}{V_w + V_f} \quad (2)$$

where V_w (microliter minute^{-1}) and V_f (microliter minute^{-1}) are the relative volumetric flow rates of the water phase and the immiscible oil phase, respectively.[26] It has been found that the size of droplets formed in T-junctions is affected mainly by the structure of the channel, the two-phase flow rates, and some physical properties such as the hydrophobicity of the channel surface.[27,28] We employed surface modification of PDMS channels using 1*H*,1*H*,2*H*,2*H*-perfluorooctyl-trichlorosilane in toluene solution to create hydrophobic PDMS channels.[29] Water-in-oil droplets in the silane-modified PDMS channels were stable and did not contaminate the channel wall compared to the effects on the unmodified PDMS channels (Figure S2 in the Supporting Information).

Parallel droplet formation in a microfluidic device requires the balancing of pressure drop both in the inlet and outlet channels and is mainly dependent on the geometry of the microfluidic device. To investigate the effect of the geometries of microfluidic devices on parallel droplet formation, we evaluated parallel droplet formation and movement in several types of microfluidic

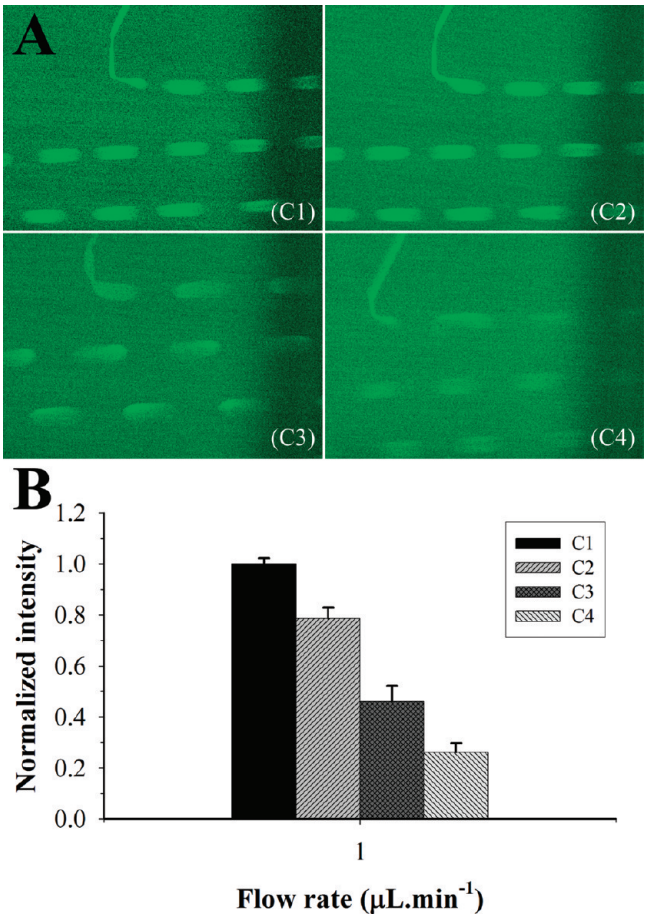

Figure 3. (A) Fluorescence images of parallel FITC droplets in four individual junctions of the microfluidic device. The droplets were stable, had a narrow size distribution: 505 ± 20 μm in diameter. (B) Normalized fluorescent intensities of over 100 droplets in the four T-junctions at $V_{\text{inlet I (FITC)}}$ = $V_{\text{inlet II (PBS)}}$ = 1.0 μL min^{-1}; $V_{\text{inlet III (PBS)}}$ = 0.5 μL min^{-1}; $V_{\text{inlet IV (oil)}}$ = 1.0 μL min^{-1}.

devices. When the geometries of all channels were the same, parallel droplets formed concomitantly in the channels with a T-junction geometry and moved without fusion. However, differences in the channel geometries resulted in loss of the ability to generate stable droplets or droplets only formed in the channels with the same geometries (Figure S3 in the Supporting Information).

Figure 3A shows fluorescence images of parallel droplet formation at the four junctions with different concentrations generated in the winding channel of the microfluidic device. The volume of droplets and the break-up mechanism in the conventional T-junction model can be controlled by adjusting the ratio of the aqueous phase flow rate (V_w) to the immiscible oil phase flow rate (V_f).[26,30,31] However, in our system, parallel droplet formation could only be controlled by adjusting the flow rate of the immiscible oil phase because we needed to maintain the aqueous flow rate at a specific, constant value to maintain an optimized concentration gradient. The fluorescence intensities of FITC droplets in PBS buffer at $V_{\text{inlet I (FITC)}}$ = $V_{\text{inlet II (PBS)}}$ = 1.0 μL min^{-1}, $V_{\text{inlet III (PBS)}}$ = 0.5 μL min^{-1}, and $V_{\text{inlet IV (oil)}}$ = 1.0 μL min^{-1} are shown in Figure 3B. Droplets generated in all four junctions were uniform in size. The normalized fluorescence intensities of FITC droplets formed at each channel from C1 to

dx.doi.org/10.1021/ac102472a |*Anal. Chem.* 2011, 83, 1603–1608

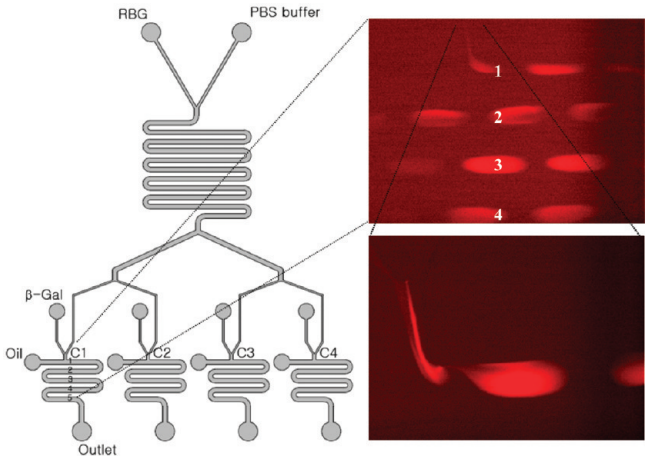

Figure 4. Scheme of the enzyme kinetic measurement of β-Gal-catalyzed hydrolysis of RBG substrate using the microfluidic device. The numbers above the channel indicate various positions that correspond to different time points for enzyme kinetic measurements. Fluorescent images of droplets containing RBG and β-Gal at magnifications of 4× and 20×, respectively.

C4 increased with corresponding values of 100%, 79%, 46%, and 26%, respectively.

In Situ Measurement of Enzyme Kinetics Using the Droplet-Based Microfluidic System. Droplets have been used to perform initial screening for a number of applications including biochemical assays, chemical reactions, and protein crystallization.[32−37] To determine the kinetic properties of an enzyme, a series of experiments in which the rate of the reaction is monitored as a function of substrate concentration are needed. This process is both time-consuming and expensive and a large sample volume is required. Although enzyme kinetic studies have been performed using droplet-based microfluidic systems,[25,38,39] our approach combines the generation of a concentration gradient with parallel droplet formation in a simple microfluidic device. Figure 4 show the performance of the device for the measurement of the enzyme kinetics of the β-Gal-catalyzed hydrolysis of the RBG substrate. A substrate concentration gradient was generated and branched into four inlet channels of a T-junction, followed by mixing with β-Gal in separated droplets. Optimized conditions for generating a linear concentration gradient and to ensure the formation of stable droplets and the movement of droplets without fusion were determined. The kinetics of the enzyme reaction was obtained by measuring the fluorescent profiles of the resorufin product. Five positions on the outlet channel were used to measure droplet fluorescent intensity; these positions are numbered from 1 to 5 in the scheme shown in Figure 4. The channel distance was converted into time using the total flow velocity obtained from the known volumetric flow rate and the cross-section of the outlet channel.[25,40,41]

A standard curve quantifying the relationship between the concentration of resorufin and its fluorescent intensity in the same microfluidic chip was used to infer the product concentration in the β-Gal enzyme reactions (Figure S4 in the Supporting Information). Figure 5A shows the kinetic traces obtained from the measurements of the fluorescence intensities of droplets at the five positions along the outlet channel for each junction, with flow rates of $V_{\text{inlet I (RBG)}} = V_{\text{inlet II (PBS)}} = 1.0\ \mu\text{L min}^{-1}$, $V_{\text{inlet III }(\beta\text{-Gal)}} = 0.5\ \mu\text{L min}^{-1}$, and $V_{\text{inlet IV (oil)}} = 1.0\ \mu\text{L min}^{-1}$. Enzyme kinetics are generally governed by the Michaelis−Menten

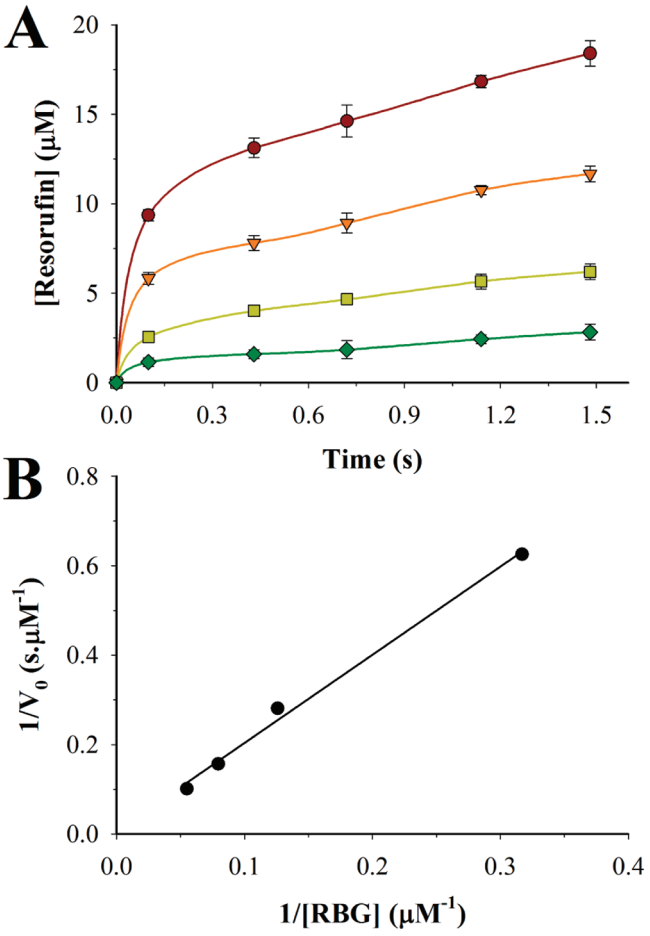

Figure 5. (A) Kinetic traces of the β-Gal-catalyzed hydrolysis of RBG at different positions along the four channels (brown ●, C1; orange ▼, C2; yellow ■, C3; green ◆, C4). Each point represents the average concentration of more than 100 droplets. (B) A Lineweaver−Burk plot obtained from part A.

equation:

$$V_o = \frac{V_{max}[S]}{K_m + [S]} \quad (3)$$

where V_o is the initial rate, [S] is the initial substrate concentration for each experiment, and the substrate concentration at which the initial rate of the product generation reaches half of the maximum rate (V_{max}) is defined as the Michaelis−Menten constant (K_m) and is recognized as one of the most important kinetic parameters of an enzyme. In the droplet-based microfluidic chip, the initial RBG substrate concentrations from channel 1 to channel 4 were inferred from the fluorescent intensities of resorufin in the four channels (Figure S5 in the Supporting Information); the fluorescent intensities of resorufin droplets in each channel were converted to resorufin concentrations using the standard curve (Figure S4 in the Supporting Information). The calculated resorufin concentrations can be used as RBG substrate concentrations because the diffusion coefficients of RBG and resorufin are similar (the diffusion coefficients of RBG and resorufin at 298 K are 4.3×10^{-10} and $4.8 \times 10^{-10}\ \text{m}^2\ \text{s}^{-1}$, respectively).[42,43] As a result, the initial concentration of RBG substrate at $V_{\text{inlet I (RBG)}} = V_{\text{inlet II (PBS)}} = 1.0\ \mu\text{L min}^{-1}$;

$V_{\text{inlet III }(\beta\text{-Gal})} = 0.5\,\mu\text{L min}^{-1}$; and $V_{\text{inlet IV (oil)}} = 1.0\,\mu\text{L min}^{-1}$ were 18, 13, 8, and 3 μM in channels C1, C2, C3, and C4, respectively. The kinetics of the β-Gal-catalyzed hydrolysis of RBG were evaluated using the Michaelis−Menten equation. Figure 5B shows the Lineweaver−Burk reciprocal plot that was used to determine the Michaelis−Menten constant, K_m, as described previously.[44] From the plot, the regression equation was $y = 1.97x + 0.01$, $R^2 = 0.99$. According to the intercept and slope of the regression equation, the K_m value for the β-Gal-catalyzed hydrolysis of RBG was estimated to be 324 μM, consistent with our previous published results (K_m = 363 μM)[9] and those of other literature (K_m = 335 ± 65 μM, 380 μM, and 450 ± 200 μM)[45,46] as well as a cuvette-based measurement (550 ± 200 μM).[47] The discrepancies between the results and those published previously may be due to the use of different substrates and measurement methods.

CONCLUSIONS

We have developed a simple droplet-based microfluidic system that combines a linear concentration gradient generated as a result of laminar diffusive mixing with parallel droplet formation in a T-junction. The device is operated using three individual syringe pumps and fluorescence microscopy and can thus be utilized in standard laboratories. Parallel droplet formation in a microfluidic device required the balancing of pressure drop both in the inlet and outlet channels and was mainly dependent on the geometry of the microfluidic device. To demonstrate the potential use of the microfluidic device, enzyme kinetic measurements of the β-Gal-catalyzed hydrolysis of RBG were performed. From the results, the K_m value for the β-Gal-catalyzed hydrolysis of RBG was estimated to be 324 μM, consistent with previous reports. We believe that the developed droplet-based microfluidic system can be applied for various chemical and biochemical analyses.

ASSOCIATED CONTENT

Supporting Information. Fluorescent images of FITC droplets and droplet formation failure in microfluidic channels, a graph quantifying the relationship between resorufin concentration and fluorescent intensity, and fluorescent intensities of resorufin in microdroplets in the four channels according to the flow rate of resorufin. This material is available free of charge via the Internet at http://pubs.acs.org.

AUTHOR INFORMATION

Corresponding Author

*Phone: +82-31-400-5202. Fax: +82-31-436-8148. E-mail: ghseong@hanyang.ac.kr.

ACKNOWLEDGMENT

This study was supported by National Research Foundation (NRF) grants funded by the Korean government (MEST) (Grant No. 2010-0024293 and Grant No. R11-2008-044-01003-0). We also acknowledge the financial support of the Ministry of Knowledge Economy (MKE) and the Korea Industrial Technology Foundation (KOTEF) through the Human Resources Training Project for Strategic Technology.

REFERENCES

(1) Teh, S.-Y.; Lin, R.; Hung, L.-H.; Lee, A. P. *Lab Chip* **2008**, *8*, 198–220.
(2) Brouzes, E.; Medkova, M.; Savenelli, N.; Marran, D.; Twardowski, M.; Hutchison, J. B.; Rothberg, J. M.; Link, D. R.; Perrimon, N.; Samuels, M. L. *Proc. Natl. Acad. Sci. U.S.A.* **2009**, *106*, 14195–14200.
(3) Chokkalingam, V.; Weidenhof, B.; Kramer, M.; Maier, W. F.; Herminghaus, S.; Seemann, R. *Lab Chip* **2010**, *10*, 1700–1705.
(4) Huebner, A.; Bratton, D.; Whyte, G.; Yang, M.; deMello, A. J.; Abell, C.; Hollfelder, F. *Lab Chip* **2009**, *9*, 692–698.
(5) Jeong, W. J.; Kim, J. Y.; Choo, J.; Lee, E. K.; Han, C. S.; Beebe, D. J.; Seong, G. H.; Lee, S. H. *Langmuir* **2005**, *21*, 3738–3741.
(6) Maerkl, S. J.; Quake, S. R. *Science* **2007**, *315*, 233–237.
(7) Bula, W. P.; Verboom, W.; Reinhoudt, D. N.; Gardeniers, H. J. G. E. *Lab Chip* **2007**, *7*, 1717–1722.
(8) Lorenz, R. M.; Fiorini, G. S.; Jeffries, G. D. M.; Lim, D. S. W.; He, M.; Chiu, D. T. *Anal. Chim. Acta* **2008**, *630*, 124–130.
(9) Bailly, M.; Yan, L.; Whitesides, G. M.; Condeelis, J. S.; Segall, J. E. *Exp. Cell Res.* **1998**, *241*, 285–299.
(10) Nelson, R. D.; Quie, P. G.; Simmons, R. L. *J. Immunol.* **1975**, *115*, 1650–1656.
(11) Boyden, S. *J. Exp. Med.* **1962**, *115*, 453–466.
(12) Dertinger, S. K. W.; Chiu, D. T.; Jeon, N. L.; Whitesides, G. M. *Anal. Chem.* **2001**, *73*, 1240–1246.
(13) Holden, M. A.; Kumar, S.; Castellana, E. T.; Beskok, A.; Cremer, P. S. *Sens. Actuators, B* **2003**, *92*, 199–207.
(14) Wu, H.; Huang, B.; Zare, R. N. *J. Am. Chem. Soc.* **2006**, *128*, 4194–4195.
(15) Kenis, P. J. A.; Ismagilov, R. F.; Whitesides, G. M. *Science* **1999**, *285*, 83–85.
(16) Jeon, N. L.; Dertinger, S. K. W.; Chiu, D. T.; Choi, I. S.; Stroock, A. D.; Whitesides, G. M. *Langmuir* **2000**, *16*, 8311–8316.
(17) Ismagilov, R. F.; Rosmarin, D.; Kenis, P. J. A.; Chiu, D. T.; Zhang, W.; Stone, H. A.; Whitesides, G. M. *Anal. Chem.* **2001**, *73*, 4682–4687.
(18) Wang, C. J.; Li, X.; Lin, B.; Shim, S.; Ming, G.-l.; Levchenko, A. *Lab Chip* **2008**, *8*, 227–237.
(19) Li Jeon, N.; Baskaran, H.; Dertinger, S. K. W.; Whitesides, G. M.; Van De Water, L.; Toner, M. *Nat. Biotechnol.* **2002**, *20*, 826–830.
(20) Georgescu, W.; Jourquin, J.; Estrada, L.; Anderson, A. R. A.; Quaranta, V.; Wikswo, J. P. *Lab Chip* **2008**, *8*, 238–244.
(21) Atencia, J.; Morrow, J.; Locascio, L. E. *Lab Chip* **2009**, *9*, 2707–2714.
(22) Gorman, B.; Wikswo, J. *Microfluid. Nanofluid.* **2008**, *4*, 273–285.
(23) Geschke, O.; Klank, H.; Tellemann, P. *Microsystem Engineering of Lab-on-a-Chip Devices*; Wiley-VCH Verlag GmbH & Co. KGaA: Weinheim, Germany, 2004.
(24) Tice, J. D.; Song, H.; Lyon, A. D.; Ismagilov, R. F. *Langmuir* **2003**, *19*, 9127–9133.
(25) Song, H.; Ismagilov, R. F. *J. Am. Chem. Soc.* **2003**, *125*, 14613–14619.
(26) Garstecki, P.; Fuerstman, M. J.; Stone, H. A.; Whitesides, G. M. *Lab Chip* **2006**, *6*, 437–446.
(27) Li, L.; Mustafi, D.; Fu, Q.; Tereshko, V.; Chen, D. L.; Tice, J. D.; Ismagilov, R. F. *Proc. Natl. Acad. Sci. U.S.A.* **2006**, *103*, 19243–19248.
(28) Gunther, A.; Jensen, K. F. *Lab Chip* **2006**, *6*, 1487–1503.
(29) Roach, L. S.; Song, H.; Ismagilov, R. F. *Anal. Chem.* **2004**, *77*, 785–796.
(30) Wang, W.-H.; Zhang, Z.-L.; Xie, Y.-N.; Wang, L.; Yi, S.; Liu, K.; Liu, J.; Pang, D.-W.; Zhao, X.-Z. *Langmuir* **2007**, *23*, 11924–11931.
(31) Link, D. R.; Anna, S. L.; Weitz, D. A.; Stone, H. A. *Phys. Rev. Lett.* **2004**, *92*, 054503.
(32) Dittrich, P. S.; Jahnz, M.; Schwille, P. *ChemBioChem* **2005**, *6*, 811–814.
(33) Shim, J.-u.; Olguin, L. F.; Whyte, G.; Scott, D.; Babtie, A.; Abell, C.; Huck, W. T. S.; Hollfelder, F. *J. Am. Chem. Soc.* **2009**, *131*, 15251–15256.

(34) Hatakeyama, T.; Chen, D. L.; Ismagilov, R. F. *J. Am. Chem. Soc.* **2006**, *128*, 2518–2519.
(35) Li, W.; Pham, H. H.; Nie, Z.; MacDonald, B.; Güenther, A.; Kumacheva, E. *J. Am. Chem. Soc.* **2008**, *130*, 9935–9941.
(36) Jia, W.; Guo, M.; Zheng, Z.; Yu, T.; Rodriguez, E. G.; Wang, Y.; Lei, Y. *J. Electroanal. Chem.* **2009**, *625*, 27–32.
(37) Zheng, B.; Gerdts, C. J.; Ismagilov, R. F. *Curr. Opin. Struct. Biol.* **2005**, *15*, 548–555.
(38) Huebner, A.; Olguin, L. F.; Bratton, D.; Whyte, G.; Huck, W. T. S.; de Mello, A. J.; Edel, J. B.; Abell, C.; Hollfelder, F. *Anal. Chem.* **2008**, *80*, 3890–3896.
(39) Song, H.; Chen, D. L.; Ismagilov, R. F. *Angew. Chem., Int. Ed.* **2006**, *45*, 7336–7356.
(40) Logan, T. C.; Clark, D. S.; Stachowiak, T. B.; Svec, F.; Fréchet, J. M. J. *Anal. Chem.* **2007**, *79*, 6592–6598.
(41) Kerby, M. B.; Legge, R. S.; Tripathi, A. *Anal. Chem.* **2006**, *78*, 8273–8280.
(42) Atalay, Y.; Verboven, P.; Vermeir, S.; Vergauwe, N.; Delport, F.; Nicolaï, B.; Lammertyn, J. *Microfluid. Nanofluid.* **2008**, *5*, 837–849.
(43) Schilling, E. A.; Kamholz, A. E.; Yager, P. *Anal. Chem.* **2002**, *74*, 1798–1804.
(44) Seong, G. H.; Heo, J.; Crooks, R. M. *Anal. Chem.* **2003**, *75*, 3161–3167.
(45) Jambovane, S.; Duin, E. C.; Kim, S.-K.; Hong, J. W. *Anal. Chem.* **2009**, *81*, 3239–3245.
(46) Hadd, A. G.; Raymond, D. E.; Halliwell, J. W.; Jacobson, S. C.; Ramsey, J. M. *Anal. Chem.* **1997**, *69*, 3407–3412.
(47) Hofmann, J.; Sernetz, M. *Anal. Chim. Acta* **1984**, *163*, 67–72.